Supplement of Biogeosciences, 18, 5539–5554, 2021
https://doi.org/10.5194/bg-18-5539-2021-supplement

Biogeosciences Open Access EGU

Supplement of

Episodic subduction patches in the western North Pacific identified from BGC-Argo float data

Shuangling Chen et al.

Correspondence to: Fei Chai (fchai@sio.org.cn)

Supplemental file

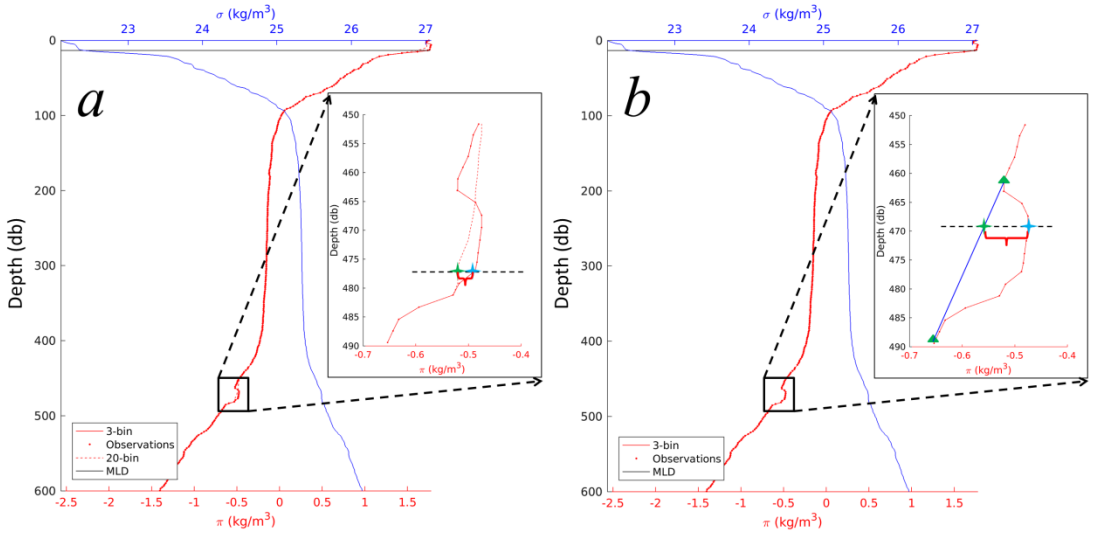

Fig. S1 A case profile (profile No. 136 of float MR2901556, box 2 in Fig. 2) with apparent subduction signals in π anomalies to illustrate the validity of our algorithm (see Methods) but the failure of the method by Llort et al. (2018) in identifying the visible subduction signal. The derived π anomaly based on 20-bin running averages is significantly dampened and too small (0.03 kg/m^3, inset in panel a) to exceed the defined threshold (0.05 kg/m^3); yet the π anomaly identified from our approach is much larger (0.07 kg/m^3, inset in panel b). The potential density and potential spicity were referenced to surface pressure.

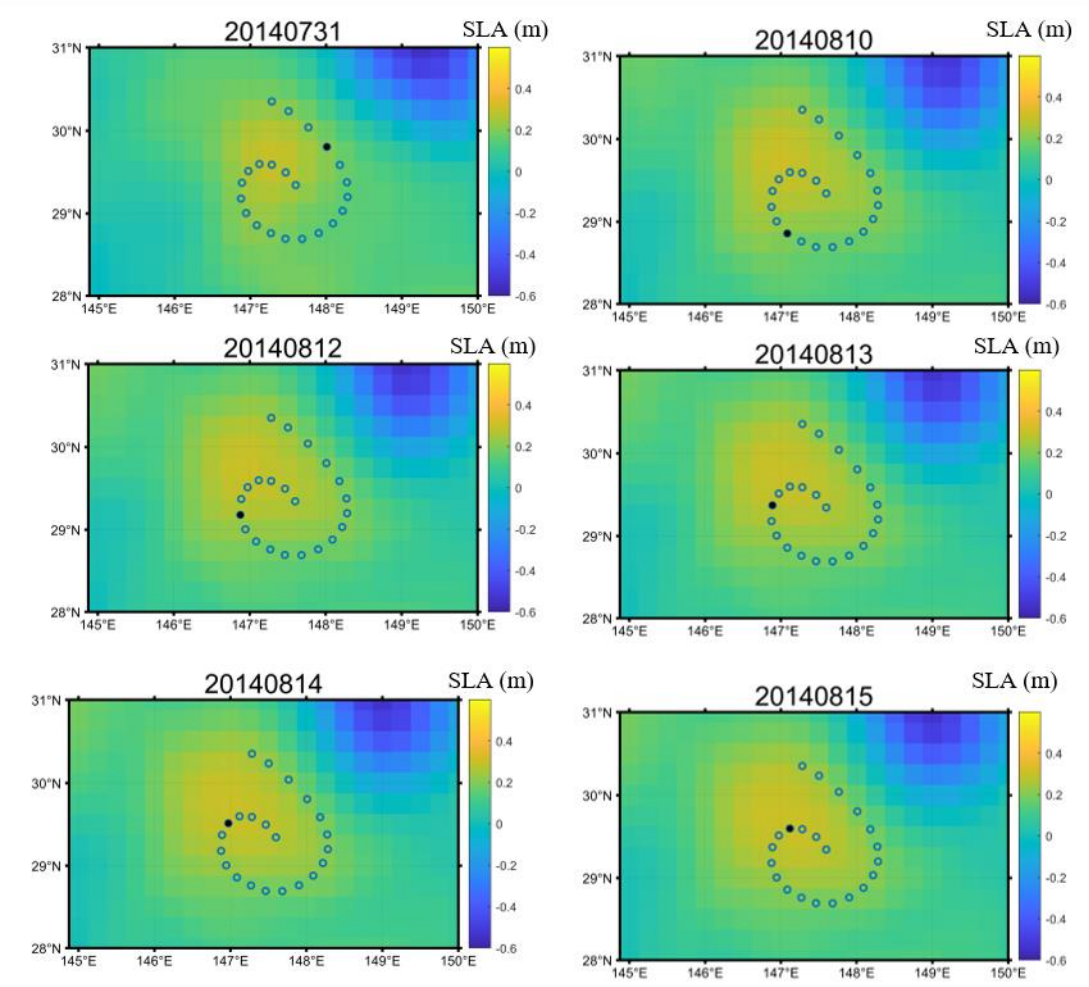

Fig. S2 The daily SLA dynamics at the observation period when episodic subduction patches were detected from float MR2901556 on July 31st, Aug 10th, and August 12th to 15th, 2014. The circled data points represent the trajectory of the float over the period, with filled circle to show the corresponding location of the float on each day.

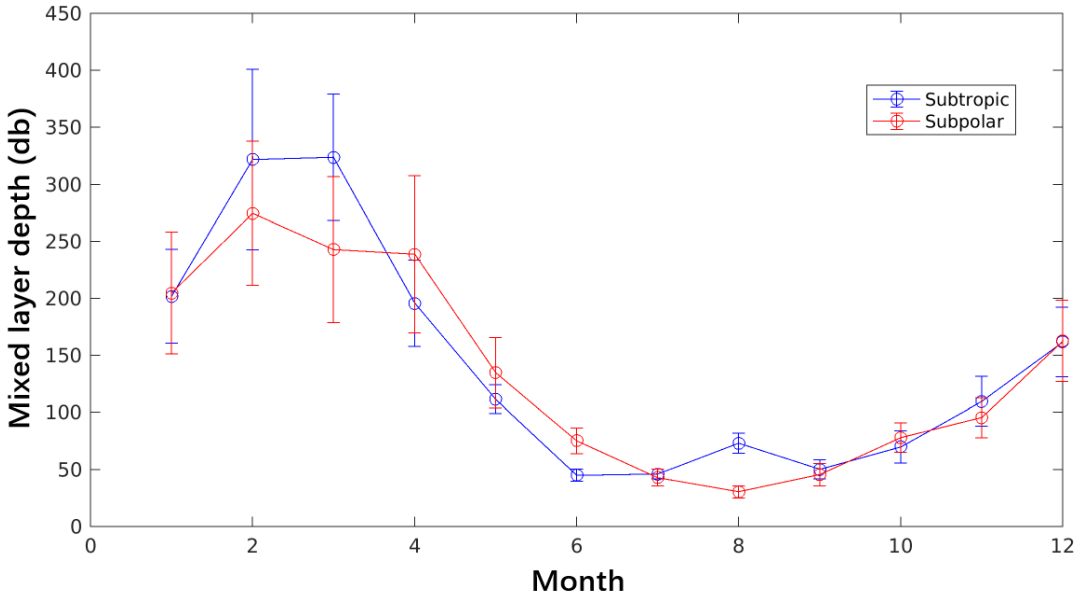

Fig. S3 The monthly variations of the maximum mixed layer depth (MLD) in the subtropical (i.e., south of 35 ° N) and subpolar (i.e., north of 35 ° N) sections of the western North Pacific, respectively, based on all the BGC-Argo profiles (N=7120, see Fig. 2). The errorbar represents one standard deviation of the mean MLD in each month.

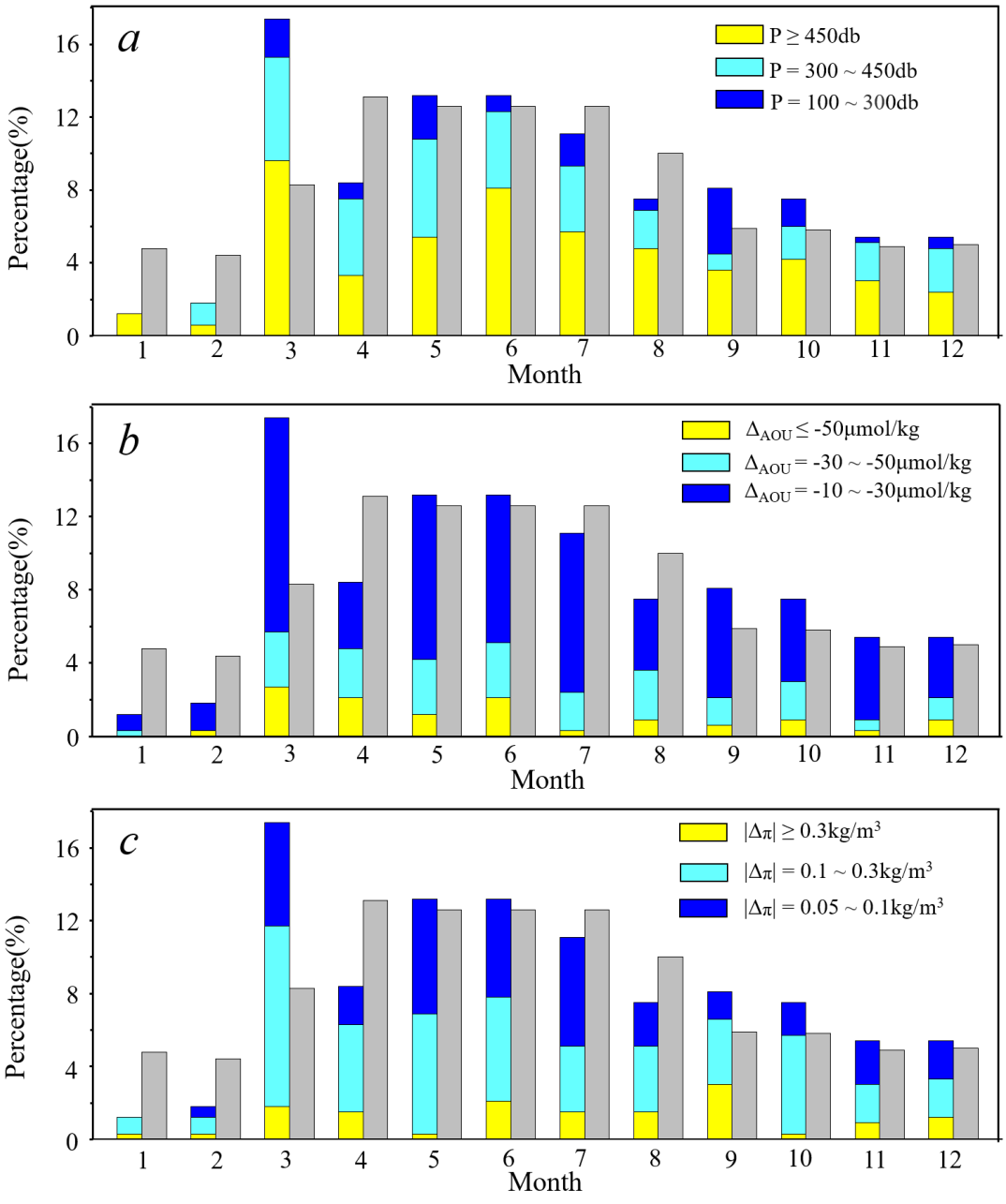

Fig. S4 Statistics of the subduction patches detected in each month, accumulated in terms of different intervals of subudction depths (a) and strengths (b and c). The grey bars in each panel represent the percentage of the number of profiles available in each month.

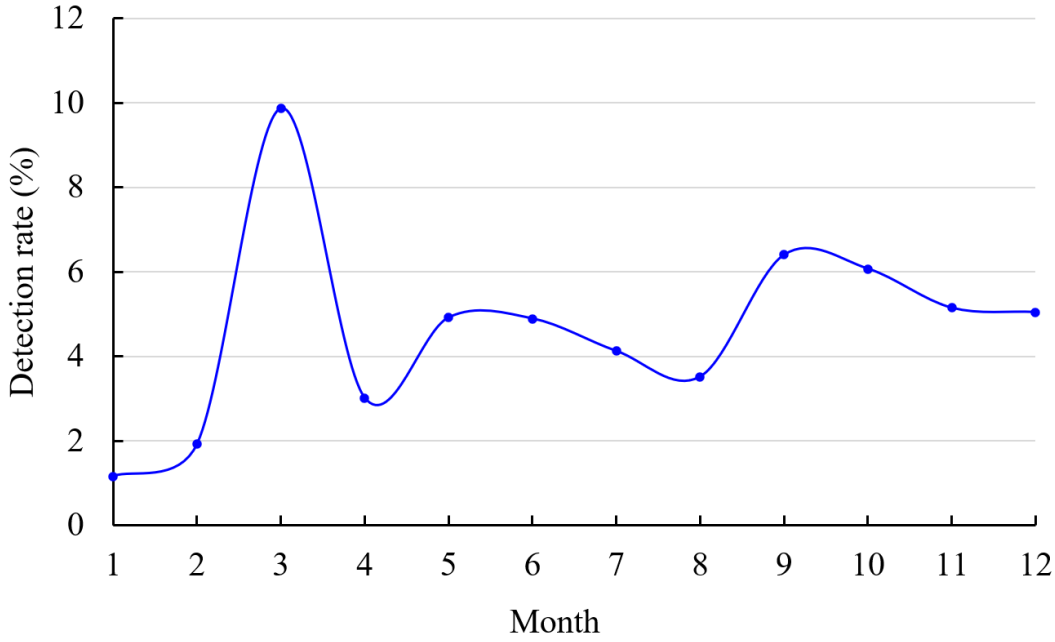

Fig. S5 The subduction detection chance (%) in each month in the western North Pacific. The subduction detection chance is defined as the ratio between the number of BGC-Argo profiles with subduction patch identified and the number of BGC-Argo profiles available in a certain month.

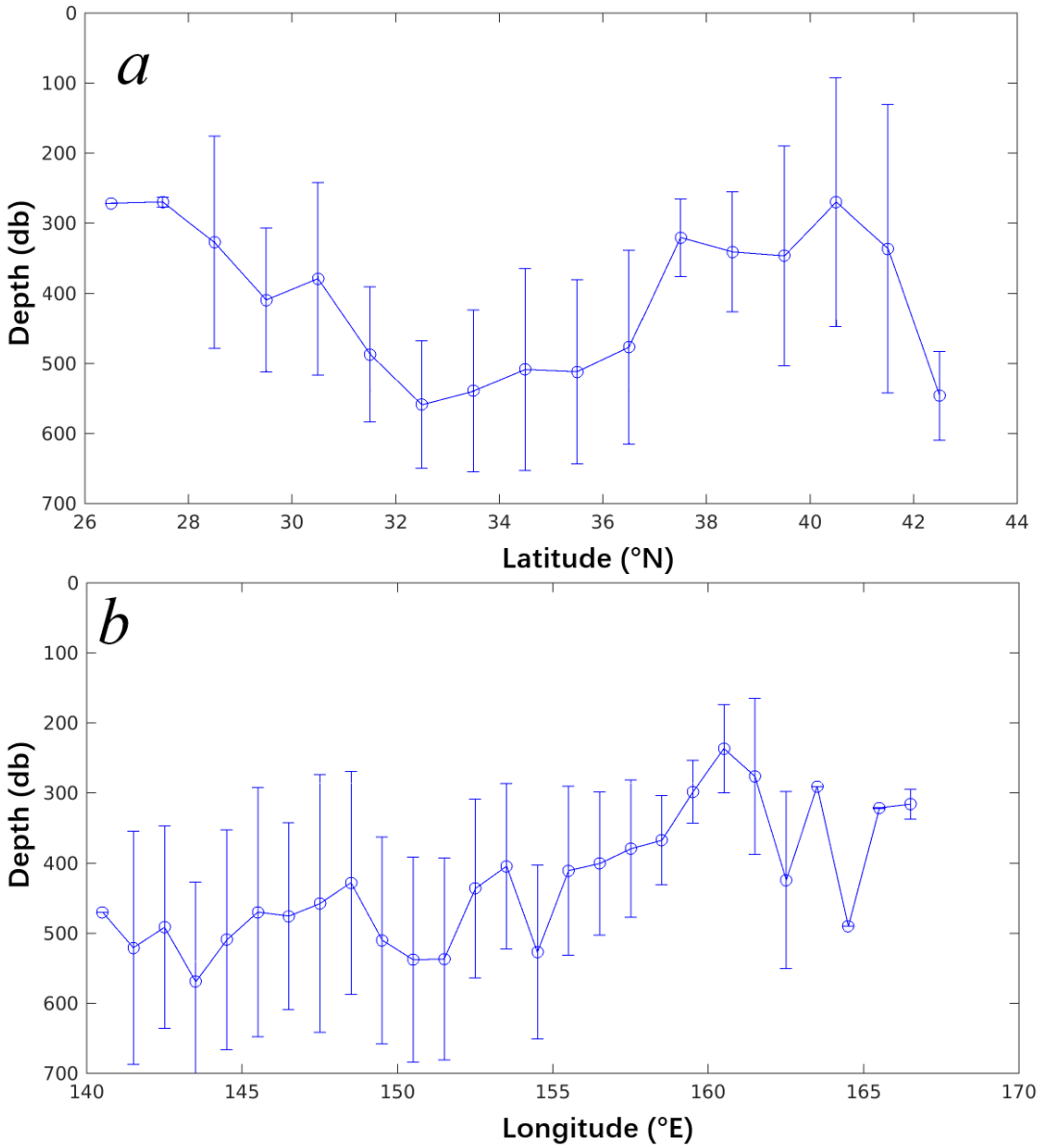

Fig. S6 Variation of the mean depths of the subduction patches observed in each 1 ° interval of latitude between 26 ° N and 44 ° N (a) and of longitude between 140 ° and 167 ° E (b). The overlaid errorbar represents one standard deviation of the depths of the subduction patches in each latitude/longitude interval.

Table S1 Sensitivity of the newly-modified algorithm to the interval of Δp by varying it between 70db and 130db, with statistics of how many more/less patches were detected, and the root mean square difference (RMSD) of the integrated Δ_{AOU} and total Δ_{π} between the new Δp and Δp of 100db. The row marked in bold refers to the Δp used in this study and the total number of subduction patches identified.

Δp (db)	Total patches	±% in total N	RMSD of $\sum\Delta_{AOU}$	RMSD of $\sum\Delta_{\pi}$

			(μmol/kg)	(kg/m^3)
Δp=130	326	-2.7%	8.9(17.7%)	0.04(16.8%)
Δp=120	329	-1.8%	6.7(18.4%)	0.04(15.9%)
Δp=110	330	-1.5%	5.1(10.8%)	0.03(11.5%)
Δp=105	329	-1.8%	4.0(6.9%)	0.03(7.3%)
Δp=103	332	-1.0%	3.8(6.6%)	0.02(6.9%)
Δp=102	334	-0.0%	3.7(5.5%)	0.01(4.5%)
Δp=101	335	0.0%	3.4(4.3%)	0.01(4.2%)
Δp=100	**335**	**0**	**0**	**0**
Δp=99	330	-1.5%	3.3(7.9%)	0.03(8.8%)
Δp=98	328	-2.0%	3.5(8.2%)	0.03(9.1%)
Δp=97	328	-2.0%	3.6(8.3%)	0.03(9.2%)
Δp=95	326	-2.7%	4.0(9.4%)	0.03((9.7%)
Δp=90	317	-5.4%	6.2(11.8%)	0.04(12.8%)
Δp=80	306	-8.7%	10.6(18.9%)	0.08 (16.4%)
Δp=70	284	-15.2%	15.6(23.4%)	0.1(22.4%)

Table S2 Statistics of the subduction patches identified in each depth interval, and the associated anomalies in AOU, DO and π on average.

Depth interval (db)	Number of subduction	Mean Δ_{AOU} (μmol/kg)	Mean Δ_{DO} (μmol/kg)	Mean Δ_{π} (kg/m^3)
100-200	8 (2.25%)	-20.89 ±6.20	30.77 ±12.39	0.33 ±0.12
200-300	41 (11.55%)	-28.80 ±16.55	34.87 ±20.84	0.13 ±0.09
300-400	87 (24.51%)	-30.34 ±16.55	37.64 ±18.70	0.18 ±0.12
400-500	69 (19.44%)	-29.30 ±17.08	35.46 ±21.05	0.18 ±0.13
500-600	57 (16.06%)	-28.94 ±17.37	37.76 ±22.17	0.20 ±0.15
600-700	60 (16.90%)	-22.92 ±12.74	29.37 ±16.80	0.15 ±0.11
700-800	13 (3.66%)	-16.50 ±8.20	19.16 ±13.61	0.18 ±0.12

Text S1: Sensitivity analysis

To investigate the robustness and representativeness of the results derived using the newly-modified algorithm (see Methods), we examined the sensitivity of the algorithm to the interval of Δp by varying it between 70db and 130db. In each test of Δp (i.e., 70db, 80db, 90db, 95db, 97db, 98db, 99db, 101db, 102db, 103db, 105db, 110db, 120db, and 130db), the total number of subduction patches identified and the corresponding strengths of Δ_{AOU} and Δ_{π} integrated for each Julian day were quantified,

and these statistics were compared with those based on Δp of 100m (following Fig. 4). Statistical measures include how many more/less patches were detected, and the RMSD of the integrated Δ_{AOU} and total Δ_{π} between the new Δp and Δp of 100m (Table S1).

In general, our choice of Δp of 100 db is reasonable and should be the most representative based on the statistics in Table S2. In each test using a new Δp, a few subudction patches failed to be identified. Specifically, for Δp of 100±3db (i.e., 97db, 98db, 99db, 101db, 102db, and 103db), less than 7 (≤ 2%) subduction patches were missed, and the resulted Δ_{AOU} and Δ_{π} show a RMSD of ≤ 3.8μmol/kg (≤ 8.3%) and ≤ 0.03 kg/m^3 (≤ 9.2%). For Δp ≤ 95db and Δp ≥ 105 db, the number of missed subduction patches were even bigger, with a maximum number of missing patches of 51 (15.2%) in case of Δp=70db. It should be noted that, although the Δp was varied at a fine vertical resolution (i.e., 1db, 5db, 10db), the vertical sampling frequency of the BGC-Argo floats changes with depth ((i.e., every 5db, 10db, and 50db for depth intervals of 0-100db, 100-500db, and 500-1000db, respectively). This coarse sampling particularly at depth is mainly responsible for the resulted changes in Δ_{AOU} and Δ_{π}.